

## Kinetics and mechanism of the reaction of sodium azide with hypochlorite in aqueous solution

Eric A. Betterton<sup>a,\*</sup>, Joe Lowry<sup>b</sup>, Robin Ingamells<sup>c,1</sup>, Brad Venner<sup>b</sup>

<sup>a</sup> Department of Atmospheric Sciences, The University of Arizona, P.O. Box 210081, Tucson, AZ 85721-0081, United States

<sup>b</sup> National Enforcement Investigations Center, U.S. EPA, Box 25227, Denver Federal Center, Denver, CO 80225, United States

<sup>c</sup> National Enforcement Investigations Center, U.S. EPA, Denver, CO, United States

### ARTICLE INFO

#### Article history:

Received 1 March 2010

Received in revised form 18 June 2010

Accepted 21 June 2010

Available online 1 July 2010

#### Keywords:

Azide

Hypochlorite

Chlorine azide

Air bag

Kinetics and mechanism

Water treatment

### ABSTRACT

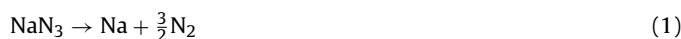
Production of toxic sodium azide ( $\text{NaN}_3$ ) surged worldwide over the past two decades to meet the demand for automobile air bag inflator propellant. Industrial activity and the return of millions of inflators to automobile recycling facilities are leading to increasing release of  $\text{NaN}_3$  to the environment so there is considerable interest in learning more about its environmental fate. Water soluble  $\text{NaN}_3$  could conceivably be found in drinking water supplies so here we describe the kinetics and mechanism of the reaction of azide with hypochlorite, which is often used in water treatment plants. The reaction stoichiometry is:  $\text{HOCl} + 2\text{N}_3^- = 3\text{N}_2 + \text{Cl}^- + \text{OH}^-$ , and proceeds by a key intermediate chlorine azide,  $\text{ClN}_3$ , which subsequently decomposes by reaction with a second azide molecule in the rate determining step:  $\text{ClN}_3 + \text{N}_3^- \rightarrow 3\text{N}_2 + \text{Cl}^-$  ( $k = 0.52 \pm 0.04 \text{ M}^{-1} \text{ s}^{-1}$ ,  $25^\circ\text{C}$ ,  $\mu = 0.1 \text{ M}$ ). We estimate that the half-life of azide would be  $\approx 15 \text{ s}$  at the point of chlorination in a water treatment plant and  $\approx 24$  days at some point downstream where only residual chlorine remains. Hypochlorite is not recommended for treatment of concentrated azide waste due to formation of the toxic chlorine azide intermediate under acidic conditions and the slow kinetics under basic conditions.

© 2010 Elsevier B.V. All rights reserved.

### 1. Introduction

The industrial production of sodium azide ( $\text{NaN}_3$ ) has surged over the past decade to meet the demand for automobile airbag inflator propellant. However it is highly toxic—even a cursory search of the Internet reveals that sodium azide toxicity is comparable to that of sodium cyanide when ingested [1]. The United States National Highway Traffic Administration (NHTSA) mandated that new passenger vehicles sold in the United States after 1996 have both driver-side and passenger-side air bags. As a result, sodium azide demand quickly rose to exceed 5 million kg in the U.S. by 1995 and has continued to rise, although the trend is now leveling off with the advent of azide-free inflators [2,3]. An inflator module typically contains compressed disks or pellets of  $\approx 60\%$  (w/w)  $\text{NaN}_3$ , blended with other ingredients, and packed into a sealed metal canister [4,5]. Each driver-side inflator contains approximately 50–80 g  $\text{NaN}_3$ , while the larger passenger-side inflator contains approximately 250 g [6]. The actual amount depends on the specific inflator, but the total installed in U.S. vehicles alone is now on the order of 50 million kg [7]. The smooth, rapid thermal decomposition charac-

teristics, the high specific nitrogen content (65 mol%), and the long shelf life make sodium azide an attractive propellant material [6,8].



Sodium azide has other uses. In the 1970s, it was used in some registered pesticide formulations, mainly for crops, and consequently discarded commercial products, off-specification product, container residues and spill residues were listed as hazardous waste by the United States Environmental Protection Agency (EPA) [9]. Lately, interest in sodium azide pesticide formulation has been revived as a replacement for methyl bromide [10]. Accordingly, sodium azide toxicity was recently on the agenda of an EPA Human Studies Internal Review Board [11]. Sodium azide is used as a preservative in certain laboratory reagents, samples and clinical fluids, and in 1989, there was an alert from the Food and Drug Administration and the Center for Disease Control (CDC) concerning the need to rinse out sodium azide preservative in certain water filters prior to use [12]. Azide can also combine with metals to form explosive metal–azide complexes. The accumulation of azide in laboratory apparatus and drains, where it can react with lead or copper-containing fixtures, has caused explosions when routine maintenance work has been attempted [13].

The azide ion is readily protonated in aqueous solution ( $\text{p}K_a = 4.65$ ) to yield volatile hydrazoic acid ( $\text{HN}_3$ ), which is itself toxic, so the atmospheric fate of azide substance is also of interest

\* Corresponding author.

E-mail address: [betterton@atmo.arizona.edu](mailto:betterton@atmo.arizona.edu) (E.A. Betterton).

<sup>1</sup> Formerly.

and has recently been described [5,14–16].



Sodium azide is highly soluble, which implies that releases into the environment could potentially migrate into sewers, streams, lakes and groundwater systems. And in fact, sodium azide has been found in groundwater at three manufacturing sites in three states, resulting in a multi-million dollar civil and criminal settlement [17].

Because of its ready availability and high toxicity, sodium azide has become a chemical of interest for the Department of Homeland Security [18], the CDC [19], and the EPA Water Supply Security Division [20]. Since it is possible that azide could be found in drinking water supplies it is of interest to know how it would behave in the presence of hypochlorite, which is commonly used in potable water treatment systems in the United States.

Oxidation by hypochlorite could also potentially be used as a treatment for much more concentrated azide-containing waste, but the results of this work lead us to recommend against such practice.

In a definitive series of mechanistic studies Margerum's group has shown that the reaction of hypochlorite with a range of nucleophiles, including  $\text{CN}^-$ ,  $\text{I}^-$ ,  $\text{Br}^-$ ,  $\text{Cl}^-$  and  $\text{SO}_3^{2-}$ , appears to proceed by way of  $\text{Cl}^+$  transfer, and not via oxygen atom transfer, as had long been thought [21–27]. Ignoring the existence of acid catalysis, the common rate law for reaction of hypochlorite with any of these nucleophiles,  $\text{X}^-$ , can be represented by:

$$\frac{-d[\text{OCl}^-]}{dt} = (k_{\text{HOCl}}[\text{HOCl}] + k_{\text{OCl}^-}[\text{OCl}^-])[\text{X}^-] \quad (3)$$

Thus, oxidation can proceed via HOCl and  $\text{OCl}^-$ , and the reaction is first-order in both hypochlorite and  $\text{X}^-$ . For all  $\text{X}^-$ , except  $\text{SO}_3^{2-}$ , the ratio  $k_{\text{HOCl}}/k_{\text{OCl}^-}$  is greater than  $10^6$ . Therefore, the HOCl route will dominate in all natural waters ( $pK_a$  HOCl = 7.31). In the case of  $\text{SO}_3^{2-}$ , the  $k_{\text{HOCl}}/k_{\text{OCl}^-}$  ratio falls to  $10^4$  and so the  $\text{OCl}^-$  route could become significant at  $\text{pH} \geq \approx 11.3$ . The value of  $k_{\text{HOCl}}$  ( $\text{M}^{-1} \text{s}^{-1}$ ) decreases with the nucleophilicity of  $\text{X}^-$ :  $\text{CN}^-$  ( $1.22 \times 10^9$ ) >  $\text{SO}_3^{2-}$  ( $7.6 \times 10^8$ ) >  $\text{I}^-$  ( $1.4 \times 10^8$ ) >  $\text{Br}^-$  ( $1.55 \times 10^3$ ) >  $\text{Cl}^-$  ( $\leq 0.16$ ) [28]. Since azide, the subject of this paper, is a pseudohalide with a nucleophilicity similar to that of bromide, it is of interest to compare the behavior of these two species in particular [29].

The first step of the HOCl route involves  $\text{Cl}^+$  transfer to an anion.



whereas the first step of the much slower  $\text{OCl}^-$  pathway formally involves an encounter between two anions, and so may be acid assisted.



Nevertheless, both pathways lead to a common intermediate, XCl, which may be quite stable, e.g., cyanogen chloride (CNCl) or bromochloride (BrCl) [28,30]. XCl is subsequently lost through either alkaline hydrolysis:



or by reaction with a second  $\text{X}^-$  [30].



In the case of  $\text{X}^- = \text{N}_3^-$ , this would lead to  $(\text{N}_3)_2$ , which would rearrange to  $3\text{N}_2$ . In fact, we will show later that this path is the dominant route for azide, unlike the halides, presumably because the production of  $\text{N}_2$  is thermodynamically so favorable.

Here we describe the kinetics and mechanism of the hypochlorite/azide reaction in aqueous solution and propose a mechanism to explain the observed rate laws. We use this information to estimate the lifetime of azide in chlorinated drinking water and to

comment on the possible treatment of concentrated aqueous azide-containing waste with hypochlorite.

## 2. Experimental

### 2.1. Materials

Water was first deionized (Calgon) and then distilled (Barnstead; conductivity  $<1 \mu\text{S cm}^{-1}$ ). Three sources of sodium azide were used (Aldrich 99.99+%; Mallinckrodt Practical; Acros 99%); no difference was observed in their electronic spectra or their kinetic behavior. We also tested two sources of sodium hypochlorite, which was either purchased (Clorox,  $\approx 0.44 \text{ M}$ ) or prepared by bubbling chlorine (Matheson, 99.99%) into 0.2 M sodium hydroxide until  $\text{Cl}_2$  could first be seen in the headspace. The excess  $\text{Cl}_2$  was immediately removed by purging with  $\text{N}_2$  to yield 0.1 M hypochlorite with  $\text{pH} \approx 7.8$ .



Again, no difference was observed in the electronic spectra or kinetic behavior of these two sources, which were stored in the dark in a refrigerator. Hypochlorite was standardized iodometrically with KI (Baker) or polarographically, with phenylarsine. The concentration was conveniently checked spectrophotometrically ( $\epsilon_{292} = 3.50 \times 10^2 \text{ M}^{-1} \text{ cm}^{-1}$ ) [22]. The speciation of halogens in water is governed by a complicated interplay between thermodynamics and kinetics, which has been described in detail [31]. Molecular chlorine ( $\text{Cl}_2$ ) is insignificant under our experimental conditions ( $<10^{-5}$  mole fraction total Cl).

Buffers with an ionic strength of 0.1 M were prepared from the following reagents:  $\text{CH}_3\text{COOH}$ ,  $\text{CH}_3\text{COONa}$ ,  $\text{Na}_2\text{HPO}_4 \cdot \text{H}_2\text{O}$ ,  $\text{NaH}_2\text{PO}_4$ ,  $\text{NaHCO}_3$ ,  $\text{NaOH}$ , from Baker;  $\text{H}_3\text{BO}_3$ , from Fisher [32]. The pH was measured at room temperature using a Radiometer TTT85 titrator and glass combination electrode (GK2401B) calibrated with Radiometer (pH 4.005, pH 10.012, pH 7.000, pH 12.450) or Ricca (pH 7.00, pH 10.00) buffers. We did not convert the measured pH values (proton activity) to  $-\log[\text{H}^+]$  values (proton concentration) so our experimentally determined constants are "mixed". We use  $K_a$  HOCl =  $4.90 \times 10^{-8}$  ( $pK_a = 7.31$ ) and  $K_a$   $\text{HN}_3 = 3.72 \times 10^{-5}$  ( $pK_a = 4.43$ ), both at 25 °C and an ionic strength,  $\mu = 0.1 \text{ M}$  [33]. These values were calculated from the available data using the Davies equation ( $\gamma = 0.8$ ) [34]. Where necessary, the effect of temperature on  $K_w$  and  $K_a$  was calculated using the appropriate enthalpies and the integrated van't Hoff equation [33].

### 2.2. Methods

#### 2.2.1. Kinetics

Kinetic studies were performed using Teflon-stoppered quartz cuvettes (1-cm) in an HP 8453 UV-visible spectrophotometer with 89090A temperature-controlled cuvette holder. (Due to the optical arrangement in this instrument the entire spectrum, rather than an absorbance at a single wavelength, is recorded each time.) The fastest reactions (low pH) were initiated by injecting the desired amount of azide into a cuvette containing the hypochlorite and rapidly mixing by inverting. In this way the entire spectrum could be recorded within 5 s of mixing and every 0.5 s thereafter. For reactions requiring several days to complete (high pH), sealed 40-mL vials containing the reactants were placed in a temperature-regulated water bath and periodically sampled to record the electronic spectrum. In most cases, the reaction was monitored for at least 5 half-lives.

The rate of reaction was studied as a function of  $[\text{N}_3^-]$  and pH (4.67–11.95). Here,  $[\text{N}_3^-] = [\text{HN}_3] + [\text{N}_3^-]$  and  $[\text{OCl}^-] = [\text{HOCl}] + [\text{OCl}^-]$ . Experiments were performed under pseudo-first-order conditions ( $[\text{N}_3^-] \gg [\text{OCl}^-]$ ), with  $[\text{OCl}^-]$

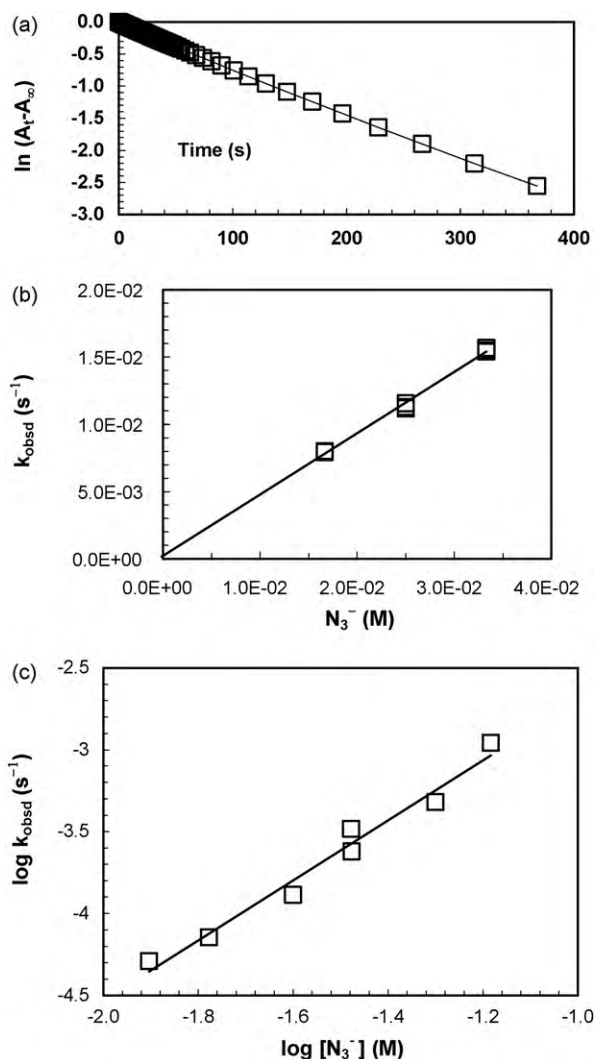


**Fig. 1.** Selected examples of the kinetic data summarized in Table 1 (25 °C,  $\mu = 0.1$  M). (a) Linear pseudo-first-order plot at pH 5.93, 1.67 mM  $[\text{OCl}_7^-]$ , 16.7 mM  $[\text{N}_3\text{T}^-]$ ; slope =  $7.07 \times 10^{-3} \text{ s}^{-1}$ ,  $t_{1/2} = 99$  s;  $r^2 = 0.9992$ . (b) Linear second-order plot; pH 5.93, slope =  $0.456 \text{ M}^{-1} \text{ s}^{-1}$ , intercept =  $2.19 \times 10^{-4} \text{ s}^{-1}$ ,  $r^2 = 0.9950$ . (c) Linear plot at high pH showing the second-order dependence on azide; pH 10.04, slope = 1.83, intercept =  $-0.865$ ,  $r^2 = 0.975$ .

normally held constant at approximately 1.67 mM and the  $[\text{N}_3\text{T}^-]$  typically ranging from a 5-fold to a 50-fold excess. The pseudo-first-order rate constant,  $k_{\text{obsd}} (\text{s}^{-1})$ , was obtained from the slope of a plot of  $\ln(A_t - A_\infty)$  vs. time, which was linear ( $r^2 > 0.99$ ) (see Fig. 1a, for example). Here,  $A_t$  = absorbance at time,  $t$ , and  $A_\infty$  = absorbance at the completion of reaction.

We chose to use two wavelengths: 292 nm where  $\text{OCl}^-$  absorbs, and 256 nm where an intermediate ( $\text{N}_3\text{Cl}$ ) absorbs (see Fig. 2 for example). Measuring the absorbance of the reactants individually before mixing (1.67 mM  $[\text{OCl}_7^-]$ , 16.4 mM  $[\text{N}_3\text{T}^-]$ , pH 4.7) showed that  $A_{256} = 0.547$  due to azide alone and  $A_{256} = 0.083$  due to hypochlorite alone so the expected initial absorbance of the mixture was 0.630. However,  $A_{256}$  was found to be nearly twice as high ( $A_{256} \approx 1.2$ ) demonstrating that an intermediate (presumably  $\text{ClN}_3$ ) with a high extinction coefficient ( $\epsilon_{256} \approx 4.3 \times 10^2 \text{ M}^{-1} \text{ cm}^{-1}$ ) was very rapidly formed.

The observed second-order rate constant ( $\text{M}^{-1} \text{ s}^{-1}$ ) was obtained from the slope of a plot of  $k_{\text{obsd}} (\text{s}^{-1})$  vs.  $[\text{N}_3\text{T}^-]$  (see Fig. 1b, for example). At pH > 8.25 the reaction was second-order in azide. In this case, the second-order rate constant was obtained from the intercept of a plot of  $\log k_{\text{obsd}}$  vs.  $\log[\text{N}_3\text{T}^-]$  (see Fig. 1c, for example).

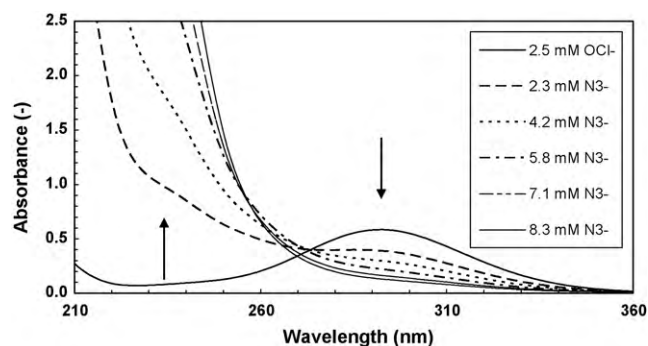


**Fig. 2.** A series of electronic spectra showing the effects of adding increasing amounts of sodium azide to 2.5 mM  $[\text{OCl}_7^-]$ . The initial  $\text{OCl}^-$  band at 292 nm disappears as azide is added. The resulting  $\text{ClN}_3$  absorbs strongly at  $\approx 210$  nm (which is masked by azide absorption at this pH), and a shoulder appears to develop at  $\approx 250$  nm.  $\text{ClN}_3$  also absorbs weakly at  $\approx 380$  nm (not shown). Isosbestic points appear to develop at  $\approx 273$  nm, and at  $\approx 256$  nm but are not sharp due to unavoidable decomposition of  $\text{ClN}_3$  that occurs during this titration (1 cm quartz cuvette; 25 °C, pH 8.2, 0.1 M borate).

Kinetic parameters derived from the linear plots were checked using non-linear regression based on the differences between observed and calculated absorbance at 256 nm and 292 nm. Mechanistic models were solved and fit to the observed data using the statistical software package “R” [35]. Chemical systems were translated into a system of differential equations, which were solved numerically using the package ODEPACK [36], which is an interface to the Fortran solver Lsoda. The advantage of non-linear regression was that it allowed different mechanistic models to be explored and fit, but was complicated by the fact that  $A_{256}$  and  $A_{292}$  are not very specific (most of the reaction species show some absorbance at these two wavelengths), and that the molar absorption coefficient of  $\text{ClN}_3$ , which is unstable in aqueous solution, has not been reported in the literature.

### 2.2.2. NMR

A JEOL 500 MHz nuclear magnetic resonance spectrometer, a 10 mm low band probe, and 10 mm glass tubes (Norell 1008-UP RB) were utilized to analyze solutions via  $^{14}\text{N}$  NMR for nitrogen containing species such as  $\text{N}_2$  ( $-67$  ppm  $\delta$ ),  $\text{NO}_2$  ( $-143$  ppm and  $-227$  ppm),  $\text{ClN}_3$  ( $-123$  ppm), and  $\text{N}_3^-$  ( $-127$  ppm and  $-278$  ppm). Chemical shift  $\delta$  values are relative to a 1 M  $\text{HNO}_3$  (JT Baker) in  $\text{D}_2\text{O}$ , the lock reference insert. Experiments were conducted with single pulses with pulse angles of  $30^\circ$  and a relaxation delay of one second. Between 128 and 32,768 scans were required for adequate signal to noise ratios. Spectra were collected from 1200 to 400 ppm, and 400 to  $-400$  ppm.

### 2.2.3. FTIR

Infrared spectra of the headspace above reaction solutions were collected with a long-path gas cell (Gemini Venus 0.5 L, 4.8 m path length) mounted in a Midac M-Series 2201-1 Fourier Transform Infrared Spectrometer using a deuterated triglycine sulfate detector at ambient temperature, with Galactic Industries Midac-Grams/32 Version 4.11 software. A pump was used to circulate headspace gas from a sealed glass reactor through an FTIR gas cell in a closed loop. Spectra were collected with 5 scans from  $650$  to  $4000 \text{ cm}^{-1}$  at a resolution of  $4 \text{ cm}^{-1}$ . Nitrous oxide was quantified relative to a 1000 ppm nitrous oxide in nitrogen gas standard (Scott specialties).

### 2.2.4. Polarography

A Princeton Applied Research Model 384C polarograph with a Model 303A cell assembly in the static mercury drop electrode mode was used to measure phenylarsonous acid for the indirect determination of hypochlorite. Polarograms were collected from

–0.3 V to –0.8 V vs. a Ag/AgCl reference electrode in the differential pulse polarography mode with a pulse amplitude of 0.1 V at a scan rate of 2 mV/s with a drop time of 1 s and a scan increment of 2 mV. Phenylarsonous acid was measured at about –0.61 V in an electrolyte consisting of a pH 4 buffer (Radiometer) containing 0.0024 M potassium iodide.

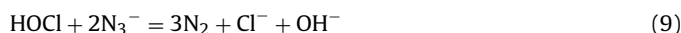
### 2.2.5. Ion chromatography

A Dionex 500 Ion Chromatography System (50  $\mu$ L sample loop; AG9 guard column; AS9 analytical column; 0.9 mM Na<sub>2</sub>CO<sub>3</sub>/0.9 mM NaHCO<sub>3</sub>; 1 mL min<sup>–1</sup>; conductivity detection) was used to determine azide, and certain possible reaction products such as nitrate, nitrite and chloride [37].

## 3. Results and discussion

### 3.1. Stoichiometry

A series of experiments described below support the following overall reaction stoichiometry.



N<sub>2</sub> evolution was quantified by water displacement from two sealed vials connected in series. A mixture of 0.132 mmol OCl<sub>7</sub><sup>–</sup> and 1 mmol [N<sub>3T</sub><sup>–</sup>] (40 mL; pH 7.0; 0.05 M phosphate) was allowed to react in a 40-mL septum-sealed vial (zero headspace), which was connected by a needle to an identical vial filled with water. As N<sub>2</sub> accumulated in the second vial, water escaped through another needle that reached to the bottom of the vial, and was collected and weighed. The reaction was allowed to proceed until gas evolution had ceased ( $\geq 4$  h). N<sub>2</sub> volume was calculated at local temperature and pressure. The N<sub>2</sub> yield was 101  $\pm$  4% of the theoretical expectations ( $\approx 12$  mL). <sup>14</sup>N NMR and FTIR spectroscopy showed that only small amounts of N<sub>2</sub>O (0.4%) and ClN<sub>3</sub> ( $\approx 0.02\%$ ) were present. In separate experiments, azide loss was shown to be quantitative within 90 min (as determined by ion chromatography) when the pH was held constant in buffered solutions (pH 4.7, 7.0, 9.0; initially [OCl<sub>7</sub><sup>–</sup>] = 15 mM, [N<sub>3T</sub><sup>–</sup>] = 2.5 mM).

Chloride production was quantified in unbuffered aqueous solution where it was found to be approximately 98% of the expected yield (initially 1:3 [OCl<sub>7</sub><sup>–</sup>]:[N<sub>3T</sub><sup>–</sup>]). The pH of these solutions increased substantially, but OH<sup>–</sup> yield was not quantified.

### 3.2. Chlorine azide (ClN<sub>3</sub>) identification

Chlorine azide is the key intermediate in our system, and since it has not been well documented in the aqueous phase it is worthwhile summarizing the evidence for its existence. Pure ClN<sub>3</sub> is an explosive liquid (b.p. 15 °C) that should not be isolated. It was first prepared in 1908 by acidification of a mixture of aqueous azide and hypochlorite [38]. It may also be prepared by chlorination of aqueous azide [39]. ClN<sub>3</sub> is reported to dissolve in water to yield a “yellow” solution before decomposing [40]. The UV–visible electronic spectrum of ClN<sub>3</sub> in *hexane* shows three bands: 211 nm (8.15  $\times 10^2$  M<sup>–1</sup> cm<sup>–1</sup>), 252 nm (2.40  $\times 10^2$  M<sup>–1</sup> cm<sup>–1</sup>), and 380 nm (8 M<sup>–1</sup> cm<sup>–1</sup>) [41].

Immediately upon mixing 1.67 mM NaN<sub>3</sub> with 1.67 mM OCl<sub>7</sub><sup>–</sup> buffered at pH 7.0, we observe a product with a spectrum similar to ClN<sub>3</sub> (in *hexane*): major bands at  $\approx 210$  nm ( $\approx 1.6 \times 10^3$  M<sup>–1</sup> cm<sup>–1</sup>) and  $\approx 250$  nm ( $\approx 4.3 \times 10^2$  M<sup>–1</sup> cm<sup>–1</sup>); and much weaker band at  $\approx 380$  nm ( $\approx 4 \times 10^1$  M<sup>–1</sup> cm<sup>–1</sup>). As will be become evident, we expect  $\approx 100\%$  ClN<sub>3</sub> formation under these conditions, although the compound decomposes quite rapidly. This compares favorably to

an estimate of  $\epsilon_{252} \approx 4.1 \times 10^2$  M<sup>–1</sup> cm<sup>–1</sup> obtained from non-linear regression analysis of the kinetic data. The ratio of the extinction coefficients at 211 nm and 252 nm in the pH 7.0 buffer solution was  $\approx 3.7$ , which is comparable to the ratio of  $\approx 3.4$  at the same wavelengths in *hexane*.

Fig. 2 shows a series of electronic spectra obtained while titrating azide into hypochlorite. The general features of ClN<sub>3</sub> can be made out but they are difficult to quantify because of unavoidable decomposition of ClN<sub>3</sub> during the titration, which is seen in the shifting isosbestic points.

<sup>14</sup>N NMR confirmed the existence of chlorine azide in the aqueous phase (33 mM NaN<sub>3</sub>, 108 mM OCl<sub>7</sub><sup>–</sup>, pH 6 phosphate, 2048 scans in 54 min) by virtue of its characteristic shift at –123 ppm. Only this peak and one for N<sub>2</sub> (–67 ppm) were observed.

FTIR analysis of the headspace showed the existence of chlorine azide in the gas phase, i.e., it is volatile. An equimolar mixture (55 mM NaN<sub>3</sub>, 55 mM OCl<sub>7</sub><sup>–</sup>, pH 6 phosphate) resulted in the headspace spectrum with the following features: chlorine azide (symmetrical N stretch near 1145 cm<sup>–1</sup> and asymmetrical N<sub>3</sub> stretch near 2075 cm<sup>–1</sup>) [42], nitrous oxide (symmetrical N<sub>2</sub>O stretch near = 1299 cm<sup>–1</sup>, asymmetrical N<sub>2</sub>O stretch near = 2236 cm<sup>–1</sup>) and hydrazoic acid (symmetrical N stretch near 1168 cm<sup>–1</sup> and asymmetrical N<sub>3</sub> stretch near 2150 cm<sup>–1</sup>).

### 3.3. Kinetics and mechanism

Based largely on Margerum’s work on the reaction of hypochlorite with the halides [22–24], we propose the following overall mechanism in which ClN<sub>3</sub> is generated by Cl<sup>+</sup> transfer to N<sub>3</sub><sup>–</sup> in the rapid first step that was too fast to follow by conventional UV–visible spectrophotometry. ClN<sub>3</sub> is subsequently lost by rate-limiting reaction with free azide.



Our kinetic data are summarized in Table 1. They are best understood by considering the reaction in three pH regimes: acid (pH  $\leq 7$ ), base (pH  $\geq 9$ ), and a transition regime (pH 8–9).

#### 3.3.1. Acidic regime

Plots of  $\ln(A_t - A_\infty)$  vs. time were linear yielding the pseudo-first-order rate constant  $k_{\text{obsd}}$  (s<sup>–1</sup>) from the slope (e.g., Fig. 1a). So the reaction is first-order in [ClN<sub>3</sub>]. Plots of  $k_{\text{obsd}}$  vs. [N<sub>3T</sub><sup>–</sup>] were also linear (i.e., the reaction is also first-order in azide) and passed through the origin, within experimental error (e.g., Fig. 1b).

The overall mechanism proposed above yields the following rate law for the observed loss of ClN<sub>3</sub> under acidic conditions.

$$\frac{-d[\text{ClN}_3]}{dt} = k_1[\text{N}_3^-][\text{ClN}_3] \quad (13)$$

$$= \alpha_1 k_1 [\text{N}_{3T}^-][\text{ClN}_3] \quad (14)$$

Here,  $\alpha_1$  is the fractional concentration of N<sub>3</sub><sup>–</sup>:

$$\alpha_1 = \left( \frac{[\text{H}^+]}{K_{\text{aHN}_3} + 1} \right)^{-1} \quad (15)$$

So the reaction rate increases with pH as  $\alpha_1$  increases to 1, i.e., at pH  $\approx 6$  (see  $k_{\text{obsd}}$  in Table 1; and Fig. 3).

The value of  $k_1$  (M<sup>–1</sup> s<sup>–1</sup>) was calculated at each pH from the observed second-order rate constant,  $k(=\alpha_1 k_1)$ , which in turn was obtained from the slope of the plot of  $k_{\text{obsd}}$  vs. [N<sub>3T</sub><sup>–</sup>] (Table 1). The average value for  $k_1 = 0.52 \pm 0.04$  M<sup>–1</sup> s<sup>–1</sup>, and is pH independent, as expected.



**Table 1**  
Summary of experimental conditions and kinetic data (25 °C;  $\mu \approx 0.1$  M). See text for definitions of  $k_{\text{obsd}}$ ,  $k_1$ ,  $K_1$  and  $n$ .

pH (buffer)	[OCl <sub>T</sub> <sup>-</sup> ] (mM)	[N <sub>3T</sub> <sup>-</sup> ] (mM)	$k_{\text{obsd}}$ (s <sup>-1</sup> )	$k_1$ (M <sup>-1</sup> s <sup>-1</sup> )	$n^d$
Acid <sup>a</sup>					
4.00 (Acetate)	1.67	17	$(1.9 \pm 0.07) \times 10^{-3}$	$(5.62 \pm 0.17) \times 10^{-1}$	1.00
		33	$(4.2 \pm 0.2) \times 10^{-3}$		
		50	$(6.9 \pm 0.1) \times 10^{-3}$		
4.67 (Acetate)	1.67	17	$(5.39 \pm 0.3) \times 10^{-3}$	$(4.99 \pm 0.17) \times 10^{-1}$	0.98
		32	$(1.05 \pm 0.02) \times 10^{-2}$		
	3.34	33	$8.9 \times 10^{-3}^c$		
5.93 (Phosphate)	1.67	17	$(7.96 \pm 0.02) \times 10^{-3}$	$(4.90 \pm 0.13) \times 10^{-1}$	0.96
		25	$(1.13 \pm 0.02) \times 10^{-2}$		
		33	$(1.55 \pm 0.01) \times 10^{-2}$		
6.97 (Phosphate)	1.67	13	$(5.21 \pm 0.1) \times 10^{-3}$	$(6.91 \pm 0.09) \times 10^{-1}$	1.05
		17	$(7.70 \pm 0.5) \times 10^{-3}$		
		25	$(1.09 \pm 0.02) \times 10^{-2}$		
		33	$(1.50 \pm 0.05) \times 10^{-2}$		
		50	$(2.33 \pm 0.03) \times 10^{-2}$		
Base <sup>b</sup>				$k_1 K_1$ (M <sup>-1</sup> s <sup>-1</sup> )	
8.20 (Borate)	1.67	17	$(7.74 \pm 0.3) \times 10^{-3}$	–	1.2
		25	$(9.34 \pm 0.2) \times 10^{-3}$		
		33	$(1.35 \pm 0.06) \times 10^{-2}$		
		50	$(2.10 \pm 0.07) \times 10^{-2}$		
9.11 (Borate)	1.67	5	$(1.16 \pm 0.02) \times 10^{-4}$	$(7.72 \pm 0.69) \times 10^{-3}$	2.11
		8.3	$(3.86 \pm 0.05) \times 10^{-4}$		
		17	$(1.87 \pm 0.05) \times 10^{-3}$		
		25	$(3.87 \pm 0.08) \times 10^{-3}$		
		33	$(5.92 \pm 0.3) \times 10^{-3}$		
10.04 (Carbonate)	1.58	13	$5.11 \times 10^{-5}$	$(8.89 \pm 2.40) \times 10^{-3}$	1.83
		17	$7.14 \times 10^{-5}$		
		25	$1.30 \times 10^{-4}$		
		33	$3.1 \pm 0.6 \times 10^{-4}$		
		50	$4.79 \times 10^{-4}$		
	1.67	50	$4.25 \times 10^{-4}^c$		
		66	$1.10 \times 10^{-3}$		
		100	$1.74 \times 10^{-3}^c$		
11.95 (Carbonate)	1.76	60	$\leq 2 \times 10^{-7}$	–	–

<sup>a</sup> Loss of ClN<sub>3</sub> monitored at 256 nm.

<sup>b</sup> Loss of OCl<sup>-</sup> monitored at 292 nm.

<sup>c</sup> Mean of two identical runs.

<sup>d</sup> Slope of the plot of  $\log k_{\text{obsd}}$  vs.  $\log [N_{3T}^-]$ , i.e., reaction order in  $[N_{3T}^-]$ .

Unfortunately, we were not able to determine  $k_{\text{HOCl}}$  for azide (Eq. (4)) because this step is too fast for our experimental system. However, based on the observation of complete formation of ClN<sub>3</sub> within the mixing time of 5 s, we estimate  $k_{\text{HOCl}}$  for N<sub>3</sub><sup>-</sup> to be  $>10^2 \text{ M}^{-1} \text{ s}^{-1}$ . This is consistent with  $k_{\text{HOCl}}$  for Br<sup>-</sup> =  $1.55 \times 10^3 \text{ M}^{-1} \text{ s}^{-1}$ .

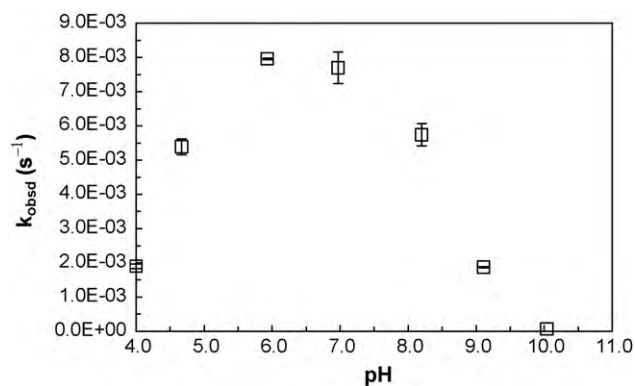


**Fig. 3.** Effect of pH on the observed first-order rate constant shown at a fixed  $[N_{3T}^-]$  of 17 mM (each point represents the mean value  $\pm 1$  standard deviation of between 3 and 7 replicates; 25 °C,  $\mu \approx 0.1$  M). Since the reaction proceeds mainly via N<sub>3</sub><sup>-</sup> and HOCl (Eqs. (11) and (12)), the rate increases from pH 4–6 as the  $\text{HN}_3 = \text{H}^+ + \text{N}_3^-$  equilibrium ( $\text{p}K_a = 4.43$ ) shifts to the right thereby generating more N<sub>3</sub><sup>-</sup>. The rate then decreases as the pH increases further because reactive hypochlorous acid is converted to inactive hypochlorite ion:  $\text{HOCl} = \text{H}^+ + \text{ClO}^-$  ( $\text{p}K_a = 7.31$ ).

### 3.3.2. Basic regime

In base, formation of ClN<sub>3</sub> is spectrophotometrically undetectable because equilibrium 11 lies far to the left. So here we monitored the loss of OCl<sup>-</sup> (not ClN<sub>3</sub>) at 292 nm. Consequently, the observed kinetic behavior changes: (a) it becomes second-order in  $[N_{3T}^-]$ ; and (b) the reaction becomes inversely dependent on  $[\text{OH}^-]$ .

Plots of  $\log k_{\text{obsd}}$  vs.  $\log [N_{3T}^-]$  were linear with a slope of  $2.0 \pm 0.2$ , i.e., second-order in N<sub>3</sub><sup>-</sup> (e.g., Fig. 1c). Plots of  $k_{\text{obsd}}$  vs.  $[\text{OH}^-]^{-1}$  were linear at fixed  $[N_{3T}^-]$ , i.e., reciprocal first-order in  $[\text{OH}^-]$  (Fig. 3).

At high pH, the amount of chloroazide that is present is small, as the equilibrium is shifted far to the left. The overall mechanism above then yields the following rate law in base.

$$\frac{-d[\text{OCl}^-]}{dt} = k_1 K_1 [\text{N}_3^-]^2 [\text{HOCl}] [\text{OH}^-]^{-1} \quad (16)$$

$$= \alpha_1 \alpha_2 k_1 K_1 [\text{N}_{3T}^-]^2 [\text{OCl}_T^-] [\text{OH}^-]^{-1} \quad (17)$$

Here,  $\alpha_2$  is the fractional concentration of HOCl:

$$\alpha_2 = \left( \frac{K_{\text{aHOCl}}}{[\text{H}^+] + 1} \right)^{-1} \quad (18)$$

In well-buffered solution (fixed  $[\text{OH}^-]$ ) with excess  $[N_{3T}^-]$ ,  $k_{\text{obsd}} = \alpha_1 \alpha_2 k_1 K_1 [\text{N}_3^-]_T^2 / [\text{OH}^-]$  (s<sup>-1</sup>) so a plot of  $\log k_{\text{obsd}}$  vs.  $\log [N_{3T}^-]$  should yield a straight line with a slope of  $n=2$  and an intercept of  $\log(\alpha_1 \alpha_2 k_1 K_1 / [\text{OH}^-])$  from which  $k_1 K_1$  can be evaluated at each pH and  $\alpha_1 \alpha_2$  (Table 1). The average

value for this lumped second-order rate constant in base is  $k_1K_1 = 7.6 \pm 1.4 \text{ M}^{-1} \text{ s}^{-1}$ ; and the average value of  $n$  was 1.97 (Table 1).

Since we have already obtained a value of  $k_1 = 0.52 \pm 0.04 \text{ M}^{-1} \text{ s}^{-1}$  we calculate  $K_1 = 7.6/0.52 = 14.6$ . This appears to be the first such estimate for an interhalogen (or pseudo-interhalogen) equilibrium constant. It proved impossible to directly determine  $K_1$  by spectrophotometric titration because  $\text{ClN}_3$  decomposed too rapidly under conditions where it could be observed.

As mentioned above, the preferred pathway for destruction of the interhalogens  $\text{ClX}$  is via reaction with  $\text{OH}^-$  (Eq. (6)) so it was of interest to examine the possibility of reaction of  $\text{ClN}_3$  with  $\text{OH}^-$  to form  $\text{HON}_3$  (hypoazidous acid), i.e.,



A non-linear kinetic model that included the  $\text{OH}^-$  step (Eq. (19)) did not improve the model fit when added to our originally proposed overall mechanism (Eqs. (10)–(12)), and actually resulted in a significantly worse fit when only the  $\text{OH}^-$  step (Eq. (19)) was in the overall mechanism. This implies that alkaline hydrolysis of  $\text{ClN}_3$  (Eq. (19)) is not a major degradation pathway. However, this is not to say that Eq. (19) is insignificant for the production of  $\text{N}_2\text{O}$  and  $\text{ONOOH}$ , as described below (Eq. (22)–(24)).

We also note that for the observed second-order dependence on azide at high pH to occur, the reaction between azide anion and  $\text{HON}_3$  would have to be the rate-limiting step, which would imply that the  $\text{HON}_3$  intermediate should be observable in solution. However, it could not be detected by UV–visible or NMR spectroscopy, lending credence to the conclusion that alkaline hydrolysis is not a significant route.

Although it does not appear to be the *major* degradation pathway in the hypochlorite/azide system, the production of trace amounts of  $\text{N}_2\text{O}$  suggests that an additional *minor* pathway might exist under certain conditions. One possible mechanism begins with hypoazidous acid ( $\text{HON}_3$ ) to yield  $\text{HON}$  that rearranges to  $\text{N}_2\text{O}$  (and which also reacts with dissolved oxygen to yield peroxyntrous acid,  $\text{ONOOH}$ ) [43].



Evidence for this minor pathway should most easily be obtained under conditions where the formation of chlorine azide consumes most of the free azide and yet where there is sufficient hydroxide for  $\text{HON}_3$  formation to proceed by Eq. (19), if only slowly. These conditions are favored in an equimolar mixture of hypochlorite and azide buffered at pH 6, where we indeed observed the formation of  $\text{N}_2\text{O}$  by headspace FTIR. UV–visible spectrophotometry of the aqueous phase showed a product with a peak at  $\approx 308 \text{ nm}$ , which is consistent with that for peroxyntrite,  $\text{ONOO}^-$ , the conjugate base of peroxyntrous acid [43]. Using the published molar absorption coefficient of  $1.67 \times 10^3 \text{ M}^{-1} \text{ cm}^{-1}$  for peroxyntrite, we estimate that about 2% of the chlorine azide is lost by this route under these conditions. This low yield is roughly consistent with the production of  $\text{N}_2\text{O}$  observed in the headspace.

Finally, we found no evidence for significant general acid catalysis in the azide/hypochlorite system, although this does not exclude the possibility of weak catalysis. For example, when doubling phosphate buffer ionic strength at pH 7,  $1.67 \text{ mM}$   $[\text{OCl}_T^-]$  and  $16.7 \text{ mM}$   $[\text{N}_3T^-]$ ,  $k_{\text{obsd}} = 7.69 \times 10^{-3} \text{ s}^{-1}$  ( $\mu = 0.05 \text{ M}$ )

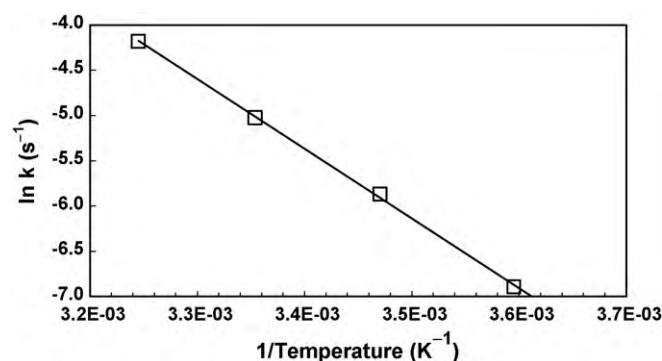


Fig. 4. Temperature dependence of the reaction between azide and hypochlorite under acidic conditions (pH 5.93, phosphate,  $\mu = 0.1 \text{ M}$ ). The pH decreases by 0.1 unit as the temperature increases from  $5^\circ\text{C}$  to  $35^\circ\text{C}$ . Slope =  $(-7.70 \pm 0.13) \times 10^3 \text{ K}$ , intercept =  $2.08 \times 10^1$ ,  $r^2 = 0.9994$ .

and  $k_{\text{obsd}} = 7.70 \times 10^{-3} \text{ s}^{-1}$  ( $\mu = 0.1 \text{ M}$ ). This is consistent with our hypothesized overall mechanism, which has no anion/anion reaction steps.

### 3.3.3. Temperature dependence

The temperature-dependence was determined from  $5^\circ\text{C}$  to  $35^\circ\text{C}$  at pH 5.93. The results are summarized in Fig. 4. The rate-limiting  $\text{ClN}_3/\text{N}_3^-$  reaction has an activation energy of  $59 \pm 1 \text{ kJ mol}^{-1}$ .

## 4. Discussion

It is of interest to use our newly acquired kinetic data to estimate the lifetime of azide in potable water treatment and distribution systems. This is governed by the chlorine concentration, for which two extremes exist. At the point of chlorination, the maximum free chlorine is dictated by its solubility ( $\approx 0.1 \text{ M}$ ) whereas further downstream, the residual chlorine level is normally about  $1.5 \mu\text{M}$  [44,45]. Assuming pH 7, and an infinite supply of chlorine (that upon dissolution yields  $\approx 50\% \text{ OCl}_T^-$ ; Eq. (8)), we estimate that the half-life of azide would be  $\approx 15 \text{ s}$  at the point of chlorination, and  $\approx 24 \text{ days}$  at some point downstream where only residual chlorine remains. In other words, azide would be quickly destroyed where chlorine is actually injected into the water, but it could remain for several weeks and become widely distributed through the system if introduced downstream of the treatment plant. We note that our work was performed with analytical grade reagents dissolved in deionized water and so the kinetics might be different in actual drinking water systems, which contain trace organics and metals such as iron, manganese and copper that could act as catalysts. Further studies using real drinking water should be conducted to verify our estimates.

Although chlorination of dilute azide in drinking water might be an effective treatment at the point of injection, chlorination is not recommended for treatment of concentrated azide-containing waste streams. Under acidic to neutral conditions, the toxic and explosive intermediate  $\text{ClN}_3$  is formed, while under basic conditions the destruction kinetics are very slow. Also, the mere acidification of azide-containing waste solutions would lead to the evolution of volatile and toxic hydrazoic acid. We note that cyanide-contaminated wastewaters can be successfully treated with chlorine under basic conditions, but this is due to the rapid hydrolysis of the intermediate cyanogen chloride. By contrast,  $\text{ClN}_3$  appears to be resistant to alkaline hydrolysis. Instead of chlorination, ozonation would appear to be a superior treatment option for azide-containing waste because it reacts very rapidly and avoids

the generation of toxic or explosive intermediates, as described in detail by one of the authors [44,45].

A detailed kinetic study of the formation of  $\text{ClN}_3$  would be of great interest but would require rapid-kinetics techniques such as stopped-flow spectrophotometry or pulsed-accelerated-flow spectrophotometry. Also, more research is needed on the chemical and toxicological properties of  $\text{ClN}_3$ . This compound is readily formed in our system and at neutral pH its concentration is limited only by the amount of azide or hypochlorite present. In particular, determination of the Henry's constant of  $\text{ClN}_3$  would be particularly useful to better evaluate its potential as a gas phase toxicant.

## Acknowledgements

We would like to thank the EPA NEIC scientists and staff, particularly John Reschel, Beth Mishalanie, Eric Nottingham and the library staff for their help. One of us, EAB, would like to thank Ms. Diana A. Love, former Director, U.S. EPA NEIC, and Mr. Les Ogden for providing the financial and administrative support that made possible his sabbatical leave from the University of Arizona.

## References

- [1] R.P. Smith, D.E. Wilcox, Toxicology of selected nitric oxide-donating xenobiotics, with particular reference to azide, *Crit. Rev. Toxicol.* 24 (1994) 355–377.
- [2] H. Fatah, Sodium azide dumping? *Chem. Week* (1996) 45.
- [3] Y. Tabani, M.E. Labib, Modeling of an air bag inflator based on combustion of methane–oxygen mixture, *Combust. Sci. Technol.* 151 (2000) 73–103.
- [4] A. Madlung, The chemistry behind the air bag—high tech in first-year chemistry, *J. Chem. Educ.* 73 (1996) 347–348.
- [5] R.E. Resh, Working knowledge. Air bags, *Sci. Am.* 274 (1996) 116.
- [6] J.M. Hitt, Automobile airbag industry toxic exposures, in: J.B. Sullivan Jr., G.R. Kreiger (Eds.), *Hazardous Materials Toxicology: Clinical Principles of Environmental Health*, Williams & Wilkins, Baltimore, 1992.
- [7] E.A. Betterton, Environmental fate of sodium azide derived from automobile airbags, in: *Critical Reviews in Environmental Science & Technology*, Taylor & Francis Ltd., 2003, pp. 423–458.
- [8] W.R. Edwards, In "Bag and Belt", *Proceedings, 1st International Akzo Symposium on Occupant Restraint Systems: Cologne, April 25–27, 1990*.
- [9] M.L. Ketchersid, M.G. Merkle, Dissipation and phytotoxicity of sodium azide in soil, *Weed Sci.* 24 (1976) 312–315.
- [10] B.M. Santos, J.P. Gilreath, T.N. Motis, J.W. Noling, J.P. Jones, J.A. Norton, Comparing methyl bromide alternatives for soilborne disease, nematode and weed management in fresh market tomato, *Crop Protect.* 25 (2006) 690.
- [11] EPA, Human Studies Review Board Meeting Report, October 24–26, 2007. <http://www.epa.gov/osa/hsrb/files/october2007hsrbfinaldraftreport3608.pdf>.
- [12] J.C. Villforth, FDA safety alert: sodium azide contamination of hemodialysis water supplies, *Am. Nephrol. Nurses' Assoc. J.* 16 (1989) 273.
- [13] NIOSH, Current Intelligence Bulletin 13 Explosive Azide Hazard, 1976. <http://www.cdc.gov/niosh/78127.13.html>.
- [14] E.A. Betterton, J.L. Robinson, Henry's law coefficient of hydrazoic acid, *J. Air Waste Manage. Assoc.* 47 (1997) 1216–1219.
- [15] H.H. Jobelius, H.-D. Scharff, Hydrazoic acid and azides, in: W. Gerhartz, Y.S. Yamamoto, F.T. Campbell, R. Pfefferkorn, J.F. Rounsaville, F. Ullmann (Eds.), *Encyclopedia of Industrial Chemistry*, VCH, Weinheim, Federal Republic of Germany, 1985, pp. 193–197.
- [16] J.J. Orlando, G.S. Tyndall, E.A. Betterton, J. Lowry, J. Lowry, Atmospheric chemistry of hydrazoic acid ( $\text{HN}_3$ ): UV absorption spectrum, HO center dot reaction rate, and reactions of the center dot N-3 radical, *Environ. Sci. Technol.* 39 (2005) 1632–1640.
- [17] EPA, TRW Vehicle Safety Systems, Inc. Hazardous Waste Settlement, 2001. <http://www.epa.gov/occaerth/resources/cases/civil/rcra/trwvssi.html>.
- [18] USA, Code of Federal Regulations. Title 6, Chapter 1, Part 27, Appendix A, 2008. <http://www.gpoaccess.gov/CFR/> or <http://www.heinonline.org>.
- [19] CDC, Emergency Preparedness & Response: Facts about Sodium Azide, 2003. <http://www.bt.cdc.gov/agent/sodiumazide/basics/facts.asp>.
- [20] EPA, Standardized Analytical Methods for Environmental Restoration Following Homeland Security Events. Revision 3.1. EPA/600/R-07/136, 2007. <http://www.epa.gov/NHSRC/pubs/600r07136.pdf>.
- [21] D.W. Johnson, D.W. Margerum, Nonmetal redox kinetics—a reexamination of the mechanism of the reaction between hypochlorite and nitrite ions, *Inorg. Chem.* 30 (1991) 4845–4851.
- [22] K. Kumar, D.W. Margerum, Kinetics and mechanism of general-acid-assisted oxidation of bromide by hypochlorite and hypochlorous acid, *Inorg. Chem.* 26 (1987) 2706–2711.
- [23] Q. Liu, D.W. Margerum, Equilibrium and kinetics of bromine chloride hydrolysis, *Environ. Sci. Technol.* 35 (2001) 1127–1133.
- [24] D.W. Margerum, K.E.H. Hartz, Role of halogen(I) cation-transfer mechanisms in water chlorination in the presence of bromide ion, *J. Environ. Monit.* 4 (2002) 20–26.
- [25] J.S. Nicoson, T.F. Perrone, K.E.H. Hartz, L. Wang, D.W. Margerum, Kinetics and mechanism of the reaction between hypochlorous acid and bromite ion, *Abstr. Pap. Am. Chem. Soc.* 224 (2002) U710–U711.
- [26] T.F. Perrone, K.E.H. Hartz, L. Wang, D.W. Margerum, Kinetics and mechanisms of the reactions of hypochlorous acid, chlorine, and chlorine monoxide with bromite ion, *Inorg. Chem.* 42 (2003) 5818–5824.
- [27] T.X. Wang, M.D. Kelley, J.N. Cooper, R.C. Beckwith, D.W. Margerum, Equilibrium, kinetic, and UV-spectral characteristics of aqueous bromine chloride, bromine, and chlorine species, *Inorg. Chem.* 33 (1994) 5872–5878.
- [28] C.M. Gerritsen, D.W. Margerum, Nonmetal redox kinetics—hypochlorite and hypochlorous acid reactions with cyanide, *Inorg. Chem.* 29 (1990) 2757–2762.
- [29] F. Basolo, Mechanisms of inorganic reactions; a study of metal complexes in solution [by] Fred Basolo and Ralph G. Pearson, 2nd ed., Wiley, New York, 1967.
- [30] K. Kumar, R.A. Day, D.W. Margerum, Atom-transfer redox kinetics—general-acid-assisted oxidation of iodide by chloramines and hypochlorite, *Inorg. Chem.* 25 (1986) 4344–4350.
- [31] F.A.F.A. Cotton, 1930–, *Advanced inorganic chemistry: a comprehensive text*, F. Albert Cotton and Geoffrey Wilkinson, 5th ed., completely rev. from the original literature. In: Wiley (Ed.), New York, c1988.
- [32] C. Long, *Biochemists' Handbook*, E.&F.N. Spon, London, 1961.
- [33] R.M. Smith, A.E. Martell, *Critical Stability Constants*, vol. 4, Plenum Press, New York, 1982.
- [34] W. Stumm, J.J. Morgan, *Aquatic Chemistry: Chemical Equilibria and Rates in Natural Waters*, 3rd ed., Wiley, New York, 1995.
- [35] R-Project, The R Project for Statistical Computing, 2009. <http://www.r-project.org/index.html>.
- [36] ODE-Pack, A Systematized Collection of ODE Solvers, 2001. <http://www.netlib.org/odepack/opkd-sum>.
- [37] OSHA, Sodium azide and hydrazoic acid in workplace atmospheres. ID-211, in, OSHA Salt Lake Technical Center, Salt Lake City, 1992.
- [38] F. Raschig, Chlorazide  $\text{N}_3\text{Cl}$  [preliminary announcement], *Berichte Der Deutschen Chemischen Gesellschaft* 41 (1908) 4194–4195.
- [39] K. Dehnicke, Darstellung Und Eigenschaften Der Azidchloride  $\text{SnCl}_3\text{N}_3$   $\text{TiCl}_3\text{N}_3$  Und  $\text{VOCl}_2\text{N}_3$ , *J. Inorganic Nucl. Chem.* 27 (1965) 809–815.
- [40] K. Dehnicke, Reactions of halogen azides, *Angew. Chem. Int. Ed.* 6 (1967) 240–246.
- [41] K. Dehnicke, P. Ruschke, Ultraviolet-spectra of halogen azides  $\text{ClN}_3$ ,  $\text{BrN}_3$  and  $\text{IN}_3$ , *Zeitschrift Fur Naturforschung Section B: J. Chem. Sci.* 33 (1978) 750–752.
- [42] A. Schulz, I.C. Tornieporthoetting, T.M. Klapotke, Experimental and theoretical vibrational studies of covalent X-N-3 azides (X = H, F, Cl, Br, I)—application of the density-functional theory and comparison with ab-initio results, *Inorg. Chem.* 34 (1995) 4343–4346.
- [43] W.A. Pryor, R. Cueto, X. Jin, W.H. Koppenol, M. Nguschwemlein, G.L. Squadrito, P.L. Uppu, R.M. Uppu, A practical method for preparing peroxyxynitrite solutions of low ionic-strength and free of hydrogen-peroxide, *Free Radic. Biol. Med.* 18 (1995) 75–83.
- [44] E.A. Betterton, D. Craig, Kinetics and mechanism of the reaction of azide with ozone in aqueous solution, *J. Air Waste Manage. Assoc.* 49 (1999) 1347–1354.
- [45] J. Hoigne, H. Bader, W.R. Haag, J. Staehelin, Rate constants of reactions of ozone with organic and inorganic-compounds in water. 3. Inorganic-compounds and radicals, *Water Res.* 19 (1985) 993–1004.